A99-16669

AIAA-99-0821

EXPERIMENTS ON SHOCK INDUCED COMBUSTION OF ISOLATED REGIONS OF HYDROGEN-OXYGEN MIXTURES

M. Valentino
Air Force Research Laboratory
Munitions Directorate
Eglin AFB, FL 32542

C. W. Kauffman, M. Sichel
Department of Aerospace Engineering
The University of Michigan
Ann Arbor, MI 48109

37th AIAA Aerospace Sciences Meeting and Exhibit
January 11-14, 1999 / Reno, NV

AIAA-99-0821

EXPERIMENTS ON SHOCK INDUCED COMBUSTION OF ISOLATED REGIONS OF HYDROGEN-OXYGEN MIXTURES

M. Valentino
Air Force Research Laboratory
Munitions Directorate
Eglin AFB, FL 32542

C. W. Kauffman†, *M. Sichel*‡
Department of Aerospace Engineering
The University of Michigan
Ann Arbor, MI 48109

ABSTRACT

The interaction of a strong plane shock wave with isolated regions of gaseous mixtures was examined through a series of shock tube experiments. Specifically, the non-uniform mixtures examined consisted of a spherical bubble of pure hydrogen or hydrogen-oxygen mixtures surrounded by either an oxygen, nitrogen or air atmosphere. Shocks in the range of Mach 1.7 to 3.7 were studied. The interaction events where recorded with high speed shadowgraphs and pressure trace recordings. No chemical reactions were observed in the interactions of shocks with strengths up to Mach 3.7 with a pure hydrogen bubble due to inadequate mixing of the reactants. In addition no reaction was observed for shocks up to Mach 3.0 interacting with a premixed stoichiometric bubble. However, shock induced combustion was observed for incident shock strengths above Mach 3.0. This demarcation between reaction and non-reaction corresponds to the classical third explosion limit for a hydrogen-oxygen mixture. This data will aid the study of the initiation and propagation of detonation waves and provide a useful set of test data for computational fluid dynamics codes involving reactive flows.

INTRODUCTION

The interactions of shock waves with fluid non-uniformities have long been studied. Typically these studies have looked at the interface of two fluids of different densities. Cases of both a shock moving from a light gas into the heavy gas and vice versa have been examined. Markstein [1,2], Richtmyer [3], Meshkov [4], Catherasoo & Sturtevant [5] and Brouillette & Sturtevant [6] examined the instabilities generated by the passage of a shock wave at planar interfaces between two different density gases. Abd-el-Fattah, et al. [7,8,9] also looked at shock waves interacting with interfaces between fluids of different densities but with an emphasis on examining the process of shock wave refraction and reflection. Haas & Sturtevant [10] extended this work by looking at shock interactions with cylindrical and spherical interfaces. Their experimental images clearly show how the passage of a shock wave over a light gas sphere deforms the sphere into a vortex ring.

The vorticity generation in these spheres due to a shock passage can easily be explained by examining the vorticity equation,

$$\rho \frac{D}{Dt}\left(\frac{\omega}{\rho}\right) = (\omega \cdot \nabla)u + \frac{1}{\rho^2}(\nabla\rho \times \nabla p) \quad (1)$$

The second term on the right shows that vorticity, ω, will be generated whenever the density and

---

Aerospace Research Engineer, Member AIAA

† Professor, Member AIAA

‡ Professor, Member AIAA

pressure gradients are not aligned. This term is known as the baroclinic torque.

The case of a shock passing over a cylindrical volume of less dense gas surrounded by a heavier gas is depicted in Figure 1(a). As the shock proceeds across the test volume vorticity is generated along the interface of the two gases. The maximum vorticity is generated when the density and pressure gradients are at ninety degrees corresponding to the top and bottom of the cylinder represented in Figure 1(b). The result is that the vorticity tends to deform the cylinder into a kidney shape shown in Figure 1(c) and eventually into a pair of vortex lines. By extension it is easily seen that a spherical bubble would tend to form into a vortex ring.

Marble et al. [11] first proposed using the induced vorticity generated at a light/heavy gas interface when subjected to a steep pressure gradient as a mechanism to enhance the mixing of the fuel and oxidizer in a scramjet. The application of this mechanism to practical scramjet engines was examined by Marble et al. [12], Waitz et al. [13] and Lee et al. [14, 15]. Conceptually, the mixing would occur by injecting the hydrogen fuel as a cylindrical jet into the supersonic airflow in the combustor. The combustor floor would be ramped such that a weak shock would be generated such that it interacted with the fuel jet leading to mixing of the fuel and oxidizer.

For the most part the research cited above has looked at the interaction of relatively weak shock waves ($\leq$ Mach 1.25) and inert gases. The thrust of the present work is to make the extension to stronger shock waves and to consider the interaction of the shocks with chemically reactive gases.

Consider spherical bubbles of pure hydrogen immersed in an oxygen atmosphere. As a shock passes over the hydrogen bubble the baroclinic torque mechanism will create a pair of vortex rings and lead to mixing of the hydrogen and oxygen. The mixing coupled with the increased pressure and temperature behind the shock wave can lead to conditions were chemical reaction might take place. For the case of premixed bubbles, no additional mixing is required however the temperature and pressure behind the shock wave must be sufficiently high to initiate a chemical reaction. The overall goal of the experiments was to gain insight into the conditions required for shock induced combustion of the isolated test volumes.

EXPERIMENTS

These experiments were conducted in the shocktube shown schematically in Figure 2. The shock tube has a rectangular cross section with internal dimensions of 64 x 38mm and is approximately 8m long. Mylar diaphragms are used to separate high-pressure helium in the driver section from the remainder of the tube. The diaphragms have a thickness of 0.2mm and are stacked together in various numbers depending on the desired shock strength. The test-section, located approximately 4.5m downstream of the diaphragms, has removable glass windows that allow a 200 x 50mm field of view.

Pulsed laser shadowgraphs were used to capture the shock interactions with the test gas spheres through the glass windows located in the test section. The pulsed laser system, shown in Figure 3, consists of a Spectra Physics argon-ion laser model 2020 coupled with a cavity-dumper model 334. A gated pulse frequency signal is sent to the cavity-dumper to control the number and frequency of images taken during a run. Typically the laser is set to pulse for 400μs with a pulse width of 9ns and a pulse separation of 2 to 20μs providing up to 35 frames of the interaction process per run. A Cordin streak camera is used to capture the images on a strip of 70mm x 300mm Kodak pan film 2484.

Along with the shadowgraph system a series of pressure switches are located upstream of the test section. These are used to give shock velocity measurements and initiate the laser pulse system. In addition to the pressure switches, two pressure transducers located inside the test section are used to provide pressure traces during the interaction process. Finally, a fast response photo detector was aimed through the test section windows at the test gas spheres. The diode used can resolve individual light flashes on the order of 1 microsecond. The detector was to record any light emissions that would indicate a chemical reaction taking place.

To prepare for an experimental run the entire shock tube driven section is first evacuated then filled with the proper gas (oxygen, nitrogen or air) at

one atmosphere. The test gas bubble was created in the following manner. The test gas (hydrogen or hydrogen-oxygen mixtures) was constrained within a soap bubble that was supported on its bottom by a post located in the middle of the test section. The soap bubbles were made with the same "Plateau's" soap solution (78% distilled water, 20% glycerin by mass 2% sodium oleate) as used by Haas and Sturtevant [10] in their experiments. The cylindrical post is stainless steel tubing with a 3.2 mm outer diameter and a 0.7 mm inner diameter. A small piece of paper with a pinprick in the center is placed on top of the post to keep the soap drop from running down the interior before the gas bubble is made. The bubbles were then made using a gas tight syringe to inject the test gas from the bottom of the post. The test section was designed with small ports directly above and below the post to allow the depositing of the soap drop and injection of the test gas. Each port had a removable cap to provide a gas tight seal. The top port's opening size was 3.2 mm. The bottom port was an extension of the support post that protruded from the bottom of the test section.

To minimize the contamination of room air into the shock tube, the driven section was initially filled with a slight overpressure of one or two psi. This excess pressure was relieved when the top and bottom ports were opened just prior to the bubble being created. All test gas bubbles created were on the order of 6 cc in volume and 19 mm in diameter. The ports were recapped as soon as the bubble was created. The diaphragms were ruptured to initiate the shock wave as quickly as possible after the bubble was created to minimize the diffusion of the test gas into the surrounding atmosphere at the soap bubble interface. Tests showed that a bubble of hydrogen initially 19 mm in diameter would shrink to 17.5 mm in 6 minutes. This corresponds to a 23 % decrease in volume. So, although the typical time from when the bubble was created until the test was conducted was less than one minute, the change in volume of the bubble could be several percent.

Finally, it should be noted that the hydrogen/oxygen test gas mixtures were made based on partial pressures. The mixtures were made by first evacuating a 500 ml sample cylinder, filling the cylinder with hydrogen at the proper partial pressure and finally filling the cylinder with oxygen until the proper total pressure was achieved. Just prior to opening the access ports on the shock tube, the contents of the sample cylinder were released into a balloon. The gas tight syringe was then inserted into the balloon and filled with the test gas hydrogen/oxygen mixture. Releasing the sample cylinder gas into the balloon shortly before creating the bubble, ensured the hydrogen and oxygen were well mixed.

DISCUSSION

Pure Hydrogen Bubble

The first series of tests looked at a shock wave interacting with a hydrogen bubble surrounded by an oxygen atmosphere. The range of shock Mach numbers investigated ran from 1.7 to 3.7. Table 1 gives a summary of these tests. This table includes the measured shock wave velocity, post shock pressure, post shock temperature and an indication of chemical reaction. It should be noted that the Mach numbers have been adjusted slightly upwards from those reported in a previous paper, Valentino et al. [16], discussing the preliminary results of these tests due to a refinement of the shock wave velocity data.

The Mach 1.7 and 2.2 tests were conducted to provide a bridge between the high Mach tests of the present work and the low Mach tests (Mach 1.05 to 1.25) of Haas and Sturtevant [10]. Also, because of the relatively benign conditions behind the Mach 1.7 shock many of the fluid dynamic features of the interaction process are more easily seen than in the images for the stronger shock cases. A detailed description of the shock-bubble interaction process for these runs can be found in Valentino, et al. [16].

Besides examining the flow field details of the interaction process, these high Mach number tests were really conducted with the goal of observing a chemical reaction between the hydrogen and oxygen. As can be seen in Table 1, most of the tests were conducted at Mach 2.9 and higher. The post shock temperature and pressure conditions behind such strong shocks would be in the range for the auto-ignition of a hydrogen-oxygen system. Post shock pressure and temperature for a Mach 2.9 shock traveling in oxygen are 9.7 atm and 750 K respectively. For a Mach 3.7 shock these values are 15.7 atm and 1050 K. The classic explosion limit data of Lewis and von Elbe [17] for a

stoichiometric hydrogen-oxygen mixture indicates that the Mach 2.9 case would be on the border of the third limit while the Mach 3.7 case would be well into the mild ignition area. So the temperature and pressures are such that ignition would occur in a stoichiometric hydrogen oxygen mixture. But, in order to see a chemical reaction for the un-premixed case at hand, the pressure and temperature must remain at an elevated level long enough for sufficient mixing to take place along with the required induction time of the H_2/O_2 reaction.

However there was no evidence of any chemical reaction when the shock interacted with a hydrogen bubble surrounded by an oxygen atmosphere from either the shadowgraph images or the photo detector signals. Figure 4 shows the shadowgraph images for the Mach 3.1 case (previously labeled Mach 2.96 in Valentino et al. [16]). The bubble does seem to remain closely coupled to the incident shock and thus should be subject to the post shock temperatures and pressures throughout the 200 μs these tests were observed. Therefore one reason that no chemical reaction occurs it that there has not been sufficient mixing of the hydrogen and oxygen despite the roll up of the bubbles into vortex rings. Unfortunately, the shadowgraph images of the present tests do not reveal any details to the interior structure of the vortices.

Premixed Hydrogen-Oxygen Bubble

Although no chemical reactions were seen for any "clean" runs with a pure hydrogen bubble, on several "bad" runs a reaction was observed. The indicators of a chemical reaction were a flash of light picked by the photo detector and strong pressure waves seen emanating from the bubble on the shadowgraph images. The "bad" runs occurred when it took an excessive amount of time between the creation of the test gas bubble and the shock or when many small bubbles of the hydrogen gas would form around the bottom of the main bubble. Both of these cases represent some degree of premixing of the hydrogen and oxygen before the shock arrives. For the long time delays, on the order of eight to ten minutes, a hydrogen bubble originally 19mm in diameter will shrink to a diameter of 16mm and will therefore have a region of premixed gas surrounding the now smaller bubble. For the cases of small bubbles forming under the main bubble it is likely the small bubbles rupture and mix quickly after the shock passes allowing ignition to occur.

Encouraged by the results of these "bad" runs, a series of controlled runs of a shock wave interacting with a premixed hydrogen-oxygen bubble were examined. The premixed bubble was surrounded by an oxygen atmosphere for the majority of the runs. However, several cases were run to look at the effects of a nitrogen or an air atmosphere.

Oxygen Atmosphere

Figure 5 shows the series of shadowgraph images taken of the Mach 3.5 shock interacting with a premixed bubble of hydrogen-oxygen at an equivalence ratio of 1.0. An oxygen atmosphere surrounds the premixed bubble. The images are taken 4 μs apart for a total of 68 μs. The interaction process appears the same as non-reacting runs up through 28 μs. However, at 32 μs a strong blast wave is seen just emerging from the top of the bubble. This wave continues to spread out from the bubble through the remaining frames and is clearly seen at 40 μs. The blast wave appears to support and accelerate the incident shock, which shows signs of curvature by the image at 52 μs. The curvature of the incident shock is more evident at 64 and 68 μs as the blast wave has grown to fill the test section from top to bottom. Smaller pressure waves can be seen between the bubble and the blast wave in the images from 48 μs to 68 μs. At 64 μs a reflected wave can be seen under the bubble from the blast wave encountering the bottom of the test section.

An estimate was made of the vertical velocity of the point where the section of the blast wave above the bubble meets normal to the incident shock. This should roughly correspond to the vertical velocity of the blast wave at this point. The velocity was measured between successive shadowgraph images starting at 40 μs and ending at 60 μs. The measured vertical velocity was roughly 500 m/s with an error of 70 m/s.

The forward-most point on the incident shock was tracked from image to image and the horizontal velocity of this point was calculated. No measurable acceleration of the shock was found through 68 μs, with the shock speed remaining constant within the 70 m/s error.

Table 2 gives a summary of the results from all the cases with a premixed hydrogen-oxygen bubble surrounded by an oxygen atmosphere. Chemical reactions were observed for all the cases with incident shock wave strength of Mach 3.1 and above. The pressure and temperature were 12 atm and 815 K respectively for the lowest strength shock, Mach 3.1, where chemical reaction was observed. Figure 6 shows these data points plotted on the explosion limit map of Lewis and von Elbe [17]. This figure shows that these conditions are in the mild ignition region to the right of the third limit. The Mach 3.0 case where no reaction was observed had a post shock pressure and temperature of 11 atm and 780 K respectively. This condition is also in the mild ignition area.

However, a one-dimensional analysis of a Mach 3.0 shock interacting with the interface between pure oxygen and a stoichiometric mixture gives the temperature and pressure inside the mixture to be quite low due to the high speed of sound of the mixture when compared to the surrounding oxygen. Even after the shock transmits through the mixture and reflects off the downstream interface the temperature and pressure of the mixture would only be 675 K and 9.5 atm respectively. These conditions are well into the non-explosion region. The same one-dimensional analysis for the Mach 3.1 case yields a mixture temperature and pressure of 700 K and 10.1 atm respectively. This is closer to the third limit yet also in the non-explosion region. But, considering that the shock-bubble interaction is not a one-dimensional problem the temperature of the bubble after the shock is probably somewhere between the temperature of the surrounding oxygen predicted by normal shock theory and that calculated for the mixture with the one-dimensional shock-interface analysis. Thus the temperatures for both cases could be shifted to the right from the one-dimensional analysis points. A situation where the Mach 3.1 case is shifted back into the mild ignition region while the Mach 3.0 case remained in the non-explosive region would be consistent with the observed results.

Nitrogen and Air Atmospheres

Table 3 gives a summary of the results from the premixed hydrogen-oxygen bubbles surrounded by either a nitrogen or air atmosphere. No chemical reactions were observed in the shadowgraphs for any of these tests. All of these tests were at Mach 3.2 to 3.5, and thus were at conditions where chemical reaction were observed for stoichiometric bubbles surrounded by oxygen. The photo detector did pick up a faint amount of light with a long delay time for one Mach 3.4 shock for a stoichiometric bubble surrounded by a nitrogen atmosphere. However a second test at the same condition revealed no light emission, indicating that this condition must be close to an explosion limit. Normal shock theory predicts the temperature and pressure behind a Mach 3.4 shock moving through nitrogen or air to be 935 K and 13.3 atm respectively. This condition is well into the mild ignition region. A one-dimensional analysis of a shock interacting with the interface between a stoichiometric bubble and a nitrogen or air atmosphere gives the temperature and pressure inside the bubble after the internally reflected shock to be 795 K and 12.5 atm. This condition is also within the mild ignition region. Both of these conditions are plotted on Figure 6. The pressures are the same and the temperatures are about 15 K colder for the same Mach 3.4 condition when an oxygen atmosphere surrounds the bubble, yet no reaction is observed for the nitrogen or air case and reaction is observed for the oxygen case.

So the question remains as to why no reaction is observed when the oxygen atmosphere surrounding the stoichiometric bubble is replaced with nitrogen or air. The answer lies in the kinetic mechanism that regulates the third limit. The governing mechanism at this limit is:

$$H + O_2 + M \leftrightarrow HO_2 + M \qquad (2)$$

Reaction (2) is chain breaking because it removes the H radical from the system. But, reaction (2) is chain breaking only if HO_2 is taken from the system before it has a chance to be involved in the reactions with O, H, or H_2. At the pressures between the second and third limits, the HO_2 radical is indeed able to reach the system boundary and thus be removed from the system. However, at the very high pressures above the third explosion limit the HO_2 radical has numerous collisions with O, H and H_2 and thus once again explosion occurs. And to complete the argument, at the third limit, the reactions removing HO_2 from the system and the reactions of HO_2 with O, H and H_2 must just balance each other. Now, consider the atmosphere surrounding the stoichiometric bubble to be the

system boundary. If that boundary is oxygen as opposed to air or nitrogen, the HO_2 radical has an increased probability of hitting an O atom in a reaction such as

$$HO_2 + O \leftrightarrow OH + O_2$$

giving a slight edge to the chain branching paths. Conversely the nitrogen or air atmospheres increase the probability the HO_2 radical is removed from the system giving a slight edge to the chain breaking mechanism. So the nitrogen or air atmospheres act in a way to move the third limit towards the right on the explosion limit plot. This is analogous to the findings of Lewis and von Elbe [17] that the third limit is shifted to the right when the diameter of the spherical vessel used in their experiments was reduced allowing the HO_2 radical to reach the walls sooner and be removed from the reactions. Thus with the temperature and pressure of the hydrogen-oxygen mixture of the present experiment somewhere between the normal shock solution and the one-dimensional analysis results, the nitrogen and air atmospheres must shift the third limit enough to the right to put the actual condition in the non-explosive region.

CONCLUSIONS

The interaction of a strong plane shock wave with isolated regions of gaseous mixtures was examined experimentally. Specifically, the non-uniform mixtures examined consisted of a spherical bubble of pure hydrogen or hydrogen-oxygen mixture surrounded by oxygen, nitrogen or air atmospheres. The goal of the experiments was to gain insight into the conditions required for shock induced combustion of the isolated test volumes.

No chemical reactions were observed in the interactions of shocks with strengths up to Mach 3.7 with a pure hydrogen sphere. The lack of chemical reactions is due to inadequate mixing of the hydrogen and oxygen in the time periods investigated. When a bubble of premixed hydrogen and oxygen were subjected to the same strength shocks chemical reaction was seen.

Shock induced combustion was observed for incident shock strengths of Mach 3.1 and above for stoichiometric mixtures of hydrogen and oxygen surrounded by an oxygen atmosphere. The chemical reaction was identified by the presence of strong blast waves appearing in the shadowgraph images. No reaction occurred when the incident shock strength dropped below Mach 3.1. This demarcation between reaction and non-reaction corresponds to the classical third explosion limit for a hydrogen-oxygen mixture.

When a nitrogen or an air atmosphere was substituted for the oxygen atmosphere surrounding the stoichiometric mixtures of hydrogen and oxygen, no chemical reactions were observed for incident shock strengths up to Mach 3.5. It is argued that the nitrogen and air act to shift the third limit to the right on the explosion limit diagram.

ACKNOWLEDGMENTS

This work was supported by the Air Force Research Laboratory, Munitions Directorate, Eglin AFB and the PALACE KNIGHT program of the United States Air Force. Additional financial support was provided by the University of Michigan, Department of Aerospace Engineering.

REFERENCES

1. Markstein, G. H. 1957 A shock tube study of flame front-pressure wave interaction. *Sixth Symp. (Intl) on Combustion*, pp 387-390. Reinhold

2. Markstein, G. H. 1964 *Nonsteady Flame Propagation*, MacMillian, NY, Chapter D.

3. Richtmyer, R.D. 1960 Taylor instability in shock acceleration of compressible fluids. *Commun. Pure Appl. Maths* **23**, 297-319

4. Meshkov, E.E. 1969 Instability of the interface of two gases accelerated by a shock wave. *Izv. AN SSSR. Mekhanika Zhidkosti i Gaza*, Vol. 4, No. 5, 151-157

5. Catherasoo, C.J. & Sturtevant, B. 1983 Shock dynamics in non-uniform media. *J. Fluid Mech.* **127**, 539-561

6. Brouillette, M. & Sturtevant, B. 1994 Experiments on the Richtmyer-Meshkov instability: single perturbations on a continuous interface. *J. Fluid Mech.* **262**, 271-291

7. Abd-el-Fattah, A.M., Henderson, L.F. & Lozzi, A. 1976 Precursor shock waves at a slow-fast gas interface. *J. Fluid Mech.* **76**, 157-176

8. Abd-el-Fattah, A.M. & Henderson, L.F. 1978a Shock waves at a fast-slow gas interface. *J. Fluid Mech.* **86**, 15-32

9. Abd-el-Fattah, A.M. & Henderson, L.F. 1978b Shock waves at a slow-fast gas interface. *J. Fluid Mech.* **89**, 79-95

10. Haas, J.F. & Sturtevant, B. 1987 Interaction of weak shock waves with cylindrical and spherical gas inhomogeneities. *J. Fluid Mech.* **181**, 41-76

11. Marble, F.E., Hendricks, G.J. & Zukoski, E.E. 1987 Progress toward shock enhancement of supersonic combustion processes. *AIAA Paper* 87-1880

12. Marble, F.E., Zukoski, E.E. & Jacobs, J. 1990 Shock enhancement and control of hypersonic mixing and combustion. *AIAA Paper* 90-1981

13. Waitz, I.A., Marble, F.E. & Zukoski, E.E. 1991 An investigation of a contoured wall injector for hypervelocity mixing augmentation. *AIAA Paper* 91-2265

14. Lee, S-H., Jeung, I-S. & Lee, S. 1996a Application of shock-enhanced mixing to circular cross-sectional combustor. *AIAA Paper* 96-0730

15. Lee, S-H., Jeung, I-S. & Yoon, Y-B. 1996b Combustion Process with shock-enhanced mixing. *AIAA Paper* 96-3131

16. Valentino, M., Kauffman, C. W. and Sichel, M., 1998 Experimental study of the mixing of reactive gases at their interface behind a shock wave. *AIAA Paper* 98-2507

17. Lewis, B. and von Elbe, G. (1987) Combustion, Flames and Explosions of Gases, 3rd Edition, Academic Press, Inc.

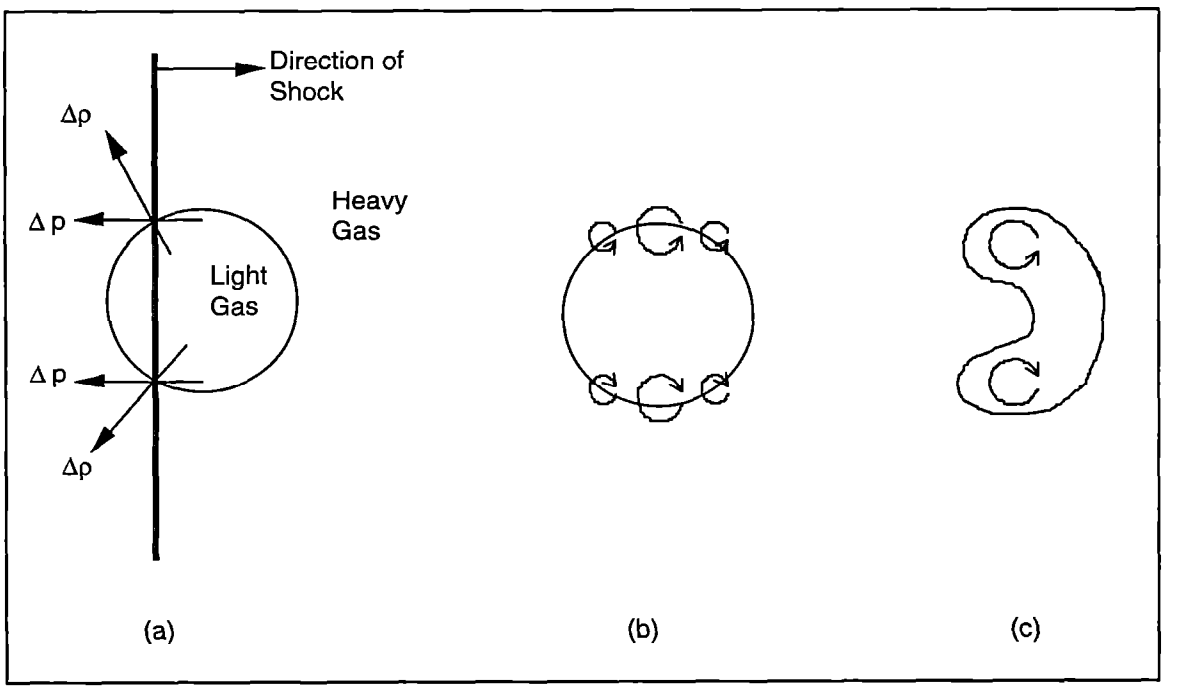

Figure 1. Shock interacting with a region of light gas: (a) Schematic of the baroclinic torque mechanism. (b) Vorticity generated along the interface. (c) Deformation of the light gas region.

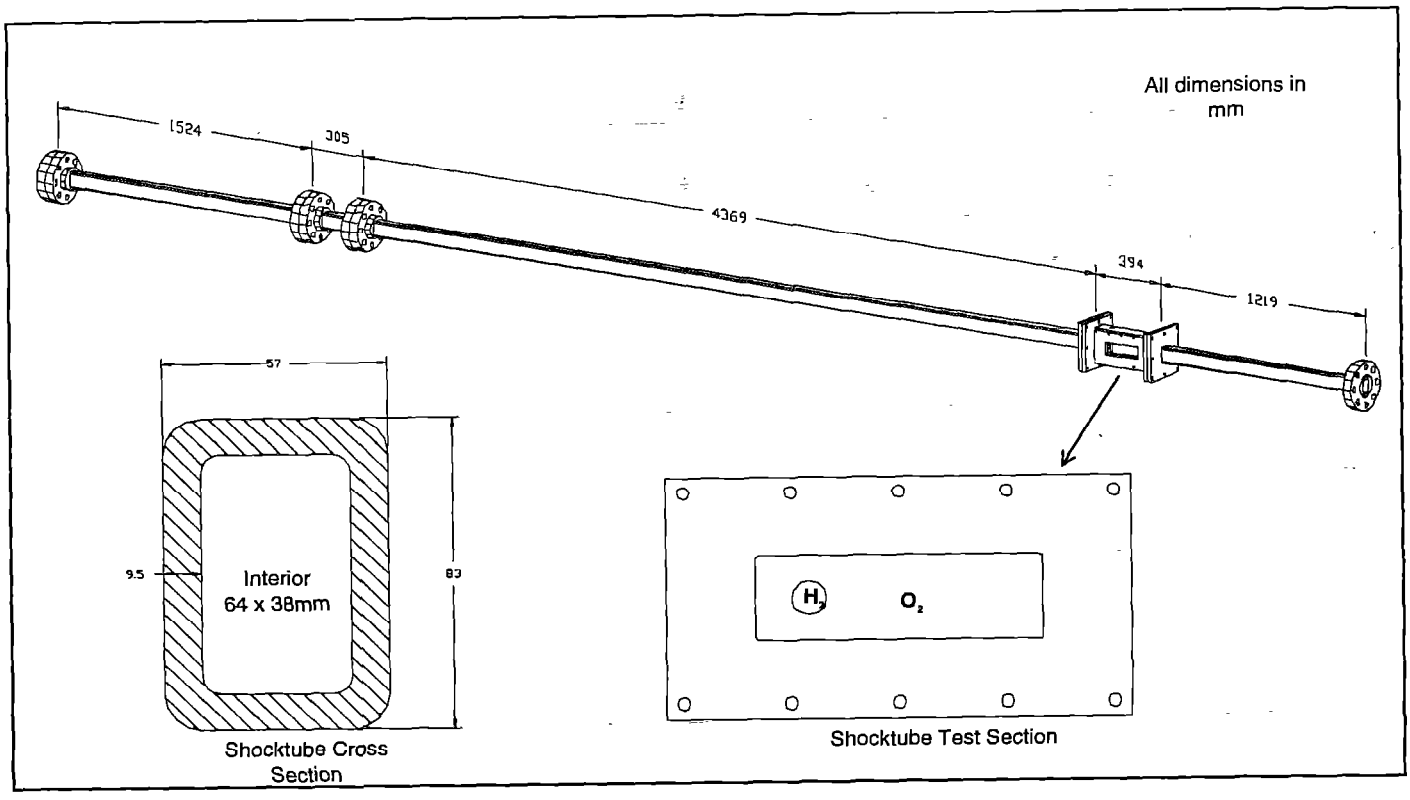

Figure 2. Shock tube schematic

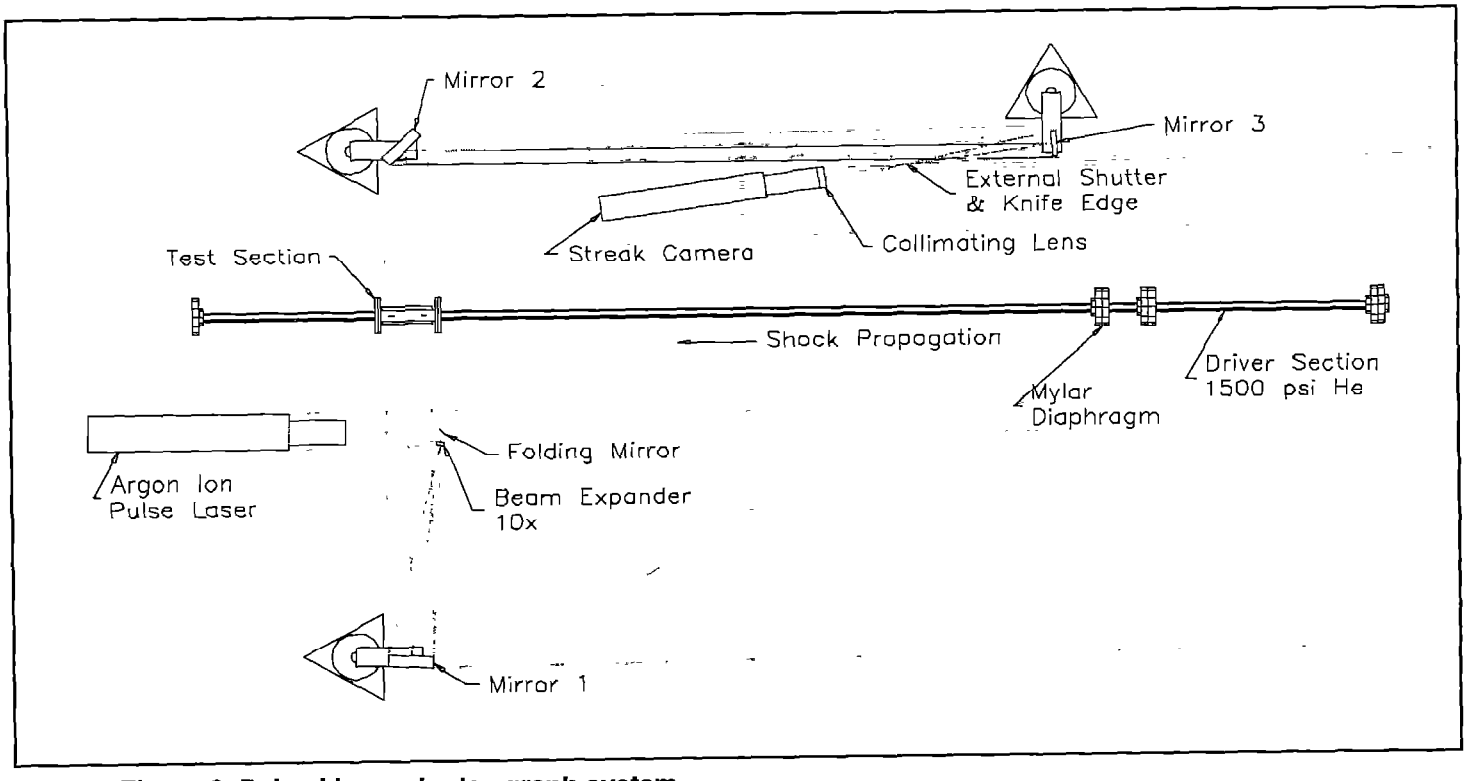

Figure 3. Pulsed laser shadowgraph system.

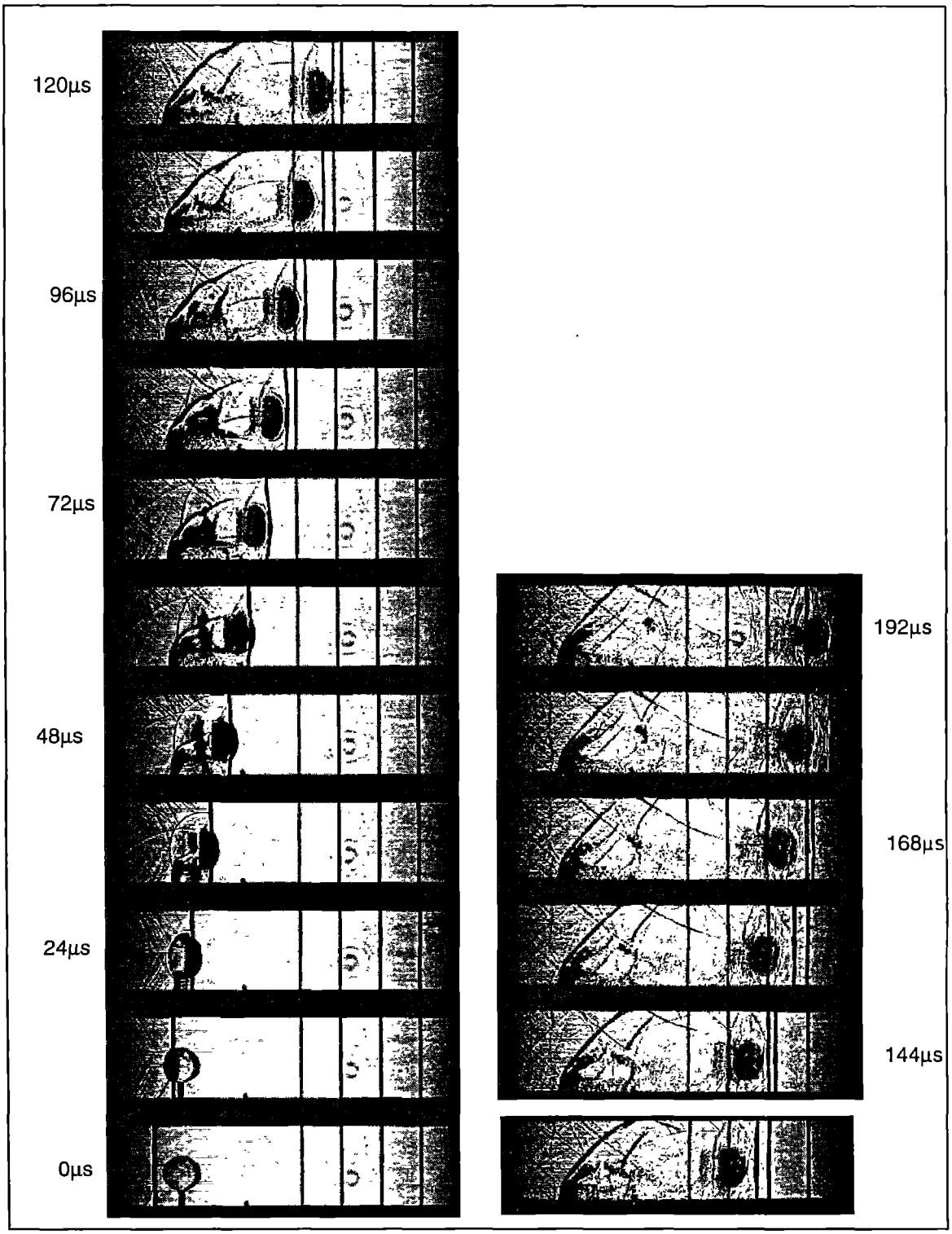

Figure 4 Shadowgraphs of a Mach 3.1 shock interacting with a spherical hydrogen bubble in an oxygen atmosphere. 12 μs between frames. S09177

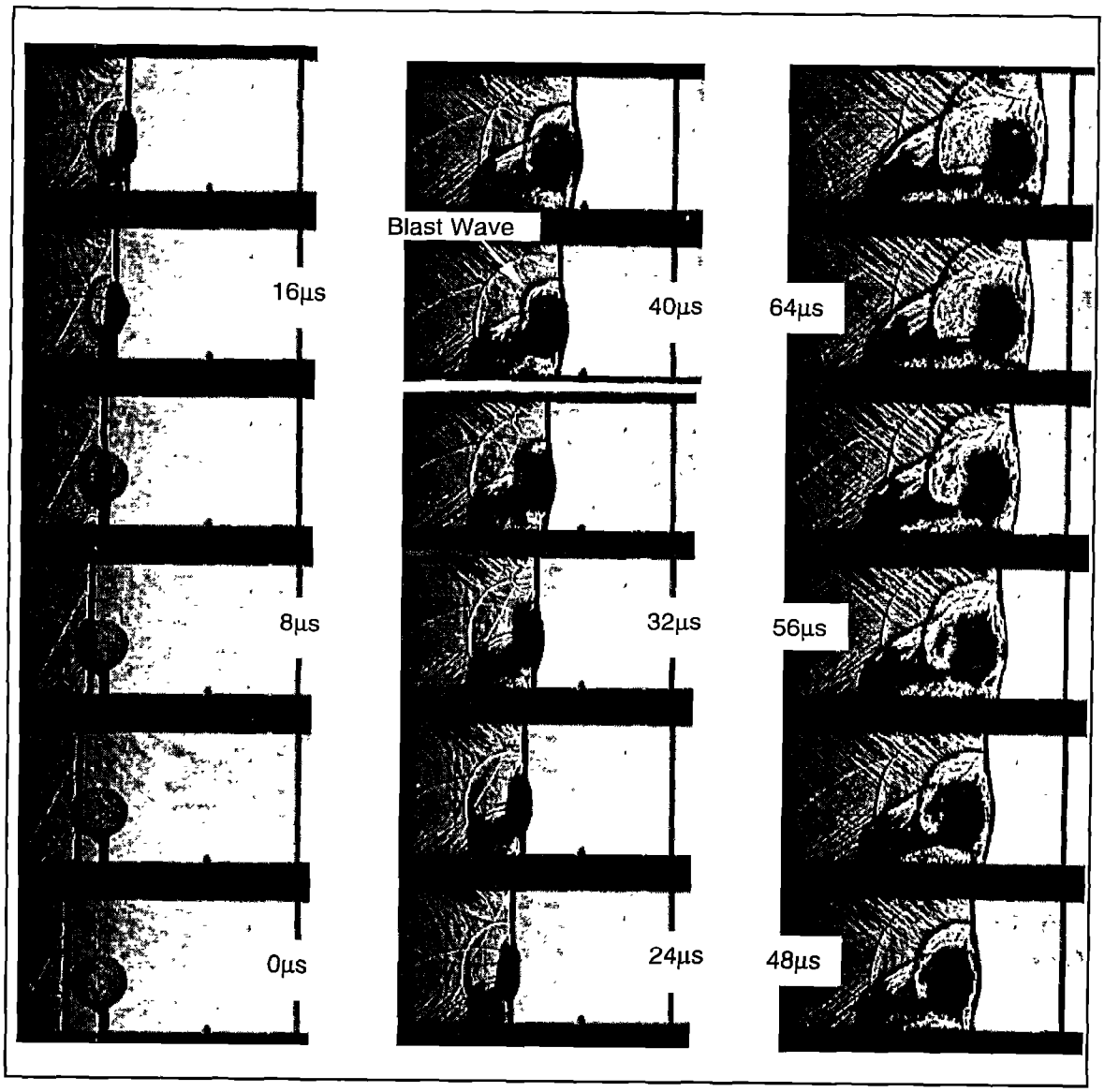

Figure 5. Shadowgraphs of a Mach 3.5 shock interacting with a spherical hydrogen/oxygen bubble, equivalence ratio of 1.0, in an oxygen atmosphere. 4μs between frames. S07138

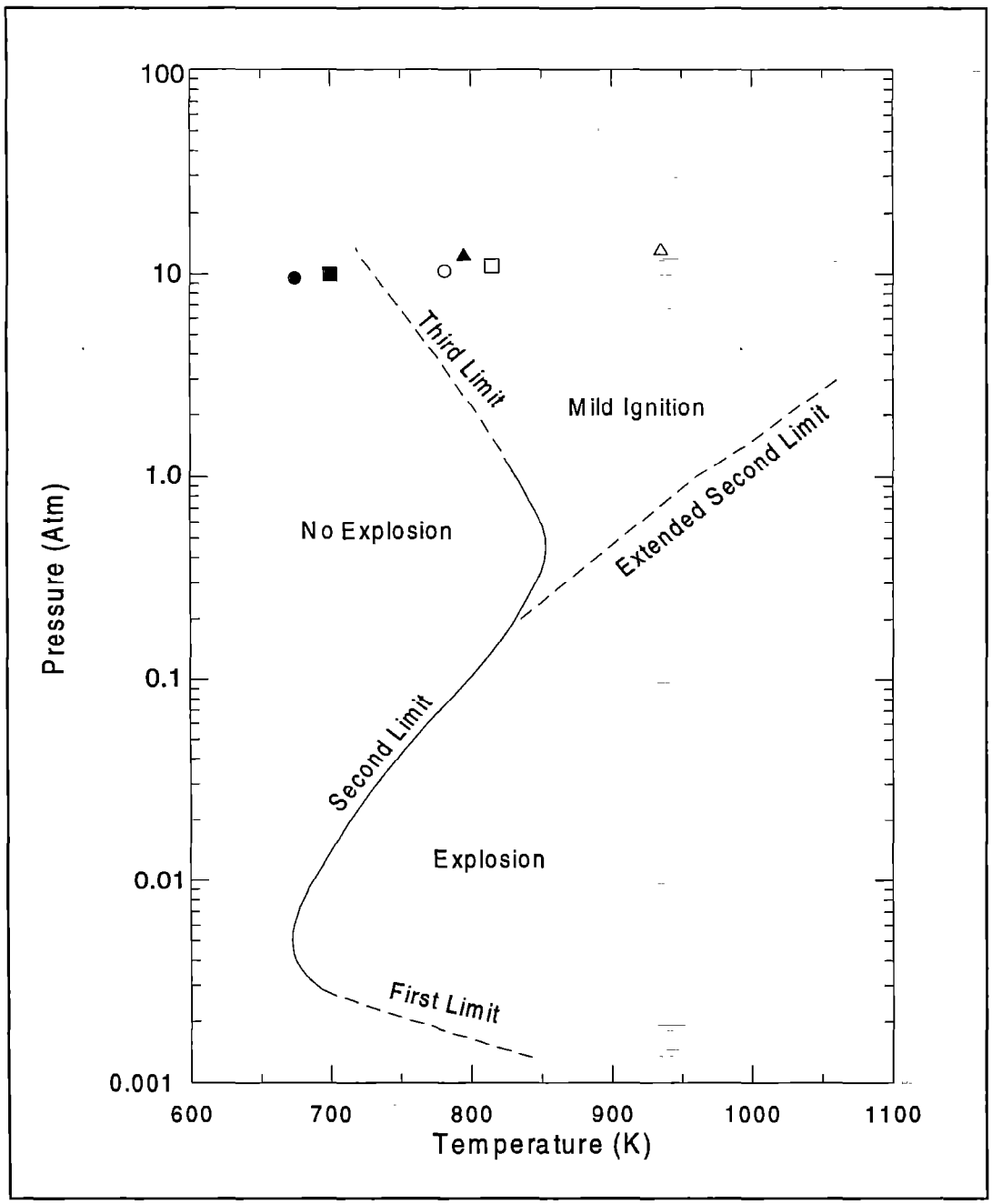

Figure 6. Explosion limits for stoichiometric H_2-O_2 mixture (Adapted from Lewis and von Elbe [17])

Circles:	**Shock Wave Mach 3.0, oxygen atmosphere**
Squares:	**Shock Wave Mach 3.1, oxygen atmosphere**
Triangles:	**Shock Wave Mach 3.4, nitrogen atmosphere**
Open symbols:	**Normal Shock Theory**
Solid symbols:	**1-D Shock-Contact Surface Analysis**

Test	Atmosphere	Test Gas	Shock Wave Mach Number[1]	Shock Wave Velocity (m/s)	Post Shock Pressure P_2 (atm)	Post Shock Temperature[2] T_2 (K)	Indication of Chemical Reaction
S12027	O_2	H_2	1.7	550	3.2	425	No
S11257	O_2	H_2	2.2	720	4.8	543	No
S12067	O_2	H_2	2.9	930	9.9	750	No
S12057	O_2	H_2	2.9	960	10.8	750	No
S09177	O_2	H_2	3.1	1020	12.2	815	No
S04238	O_2	H_2	3.6	1170	15.3	1110	No
S04268	O_2	H_2	3.7	1210	15.3	1150	No

Table 1 Summary of Results from the Pure Hydrogen Bubble Tests

[1] Speed of sound used for given atmosphere: O2 - 326 m/s

[2] Calculated from normal shock relations based on Mach and given atmosphere ideal gas properties

AIAA-99-0821

Test	Atmosphere	Test Gas Equivalence Ratio ϕ	Shock Wave Mach Number[1]	Shock Wave Velocity (m/s)	Post Shock Pressure P_2 (atm)	Post Shock Temperature[2] T_2 (K)	Indication of Chemical Reaction
S04208	O_2	1.0	3.0	970	10.9	780	No
S04028	O_2	1.0	3.1	1010	11.9	815	Yes
S07168	O_2	1.0	3.3	1080	12.6	890	Yes
S04288	O_2	1.0	3.5	1140	13.9	970	Yes
S07138	O_2	1.0	3.5	1140	13.6	970	Yes

Table 2 Summary of Results: Premixed Hydrogen-Oxygen Bubble in an Oxygen Atmosphere

[1]Speed of sound used for given atmosphere: O2 - 326 m/s

[2]Calculated from normal shock relations based on Mach and given atmosphere ideal gas properties

AIAA-99-0821

Test	Atmosphere	Test Gas Equivalence Ratio ϕ	Shock Wave Mach Number[1]	Shock Wave Velocity (m/s)	Post Shock Pressure P_2 (atm)	Post Shock Temperature[2] T_2 (K)	Indication of Chemical Reaction
S08028 1	N_2	1.0	3.2	1130	12.6	860	No[3]
S07218	N_2	1.0	3.4	1210	13.9	935	No
S07228	N_2	1.0	3.4	1200	13.9	935	Yes[4]
S08058	Air	1.0	3.4	1180	14.3	935	No
S08048	Air	1.0	3.5	1190	14.3	975	No

Table 3 Summary of Results: Premixed Hydrogen-Oxygen Bubble in Nitrogen or Air Atmosphere

[1]Speed of sound used for given atmosphere: N2 - 350 m/s, Air - 344 m/s

[2]Calculated from normal shock relations based on Mach and given atmosphere ideal gas properties

[3]Shadowgraphs not available, but photodetector did not pick up any light

[4]No blast wave seen on shadowgraph images, but a small amount of light picked up by photodetector

AIAA-99-0821